



Tuning Catalytic Selectivity in Cascade Reactions by Light Irradiation

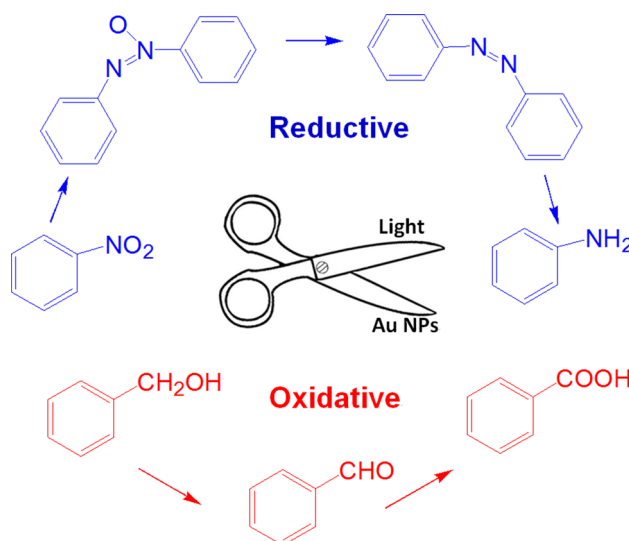
Xingguang Zhang¹ · Jianfeng Yao¹ · Xuebin Ke²

Received: 26 November 2017 / Accepted: 5 February 2018
© Springer Science+Business Media, LLC, part of Springer Nature 2018

Abstract

Selectivity of cascade redox reactions: the reduction of nitrobenzene to azoxybenzene and then to azobenzene and the oxidation of benzyl alcohol to benzaldehyde and then to benzoic acid, is discovered to be tuneable via light irradiation over plasmonic gold photocatalysts. The representative photocatalyst of Au/CeO₂ was characterized by TEM, EDX, UV–Vis and XPS to determine its morphology, elemental composition, photo absorptivity and oxidation state of gold. The catalytic test results demonstrate that the net contribution of light irradiation correlates with the ability of incident light to excite electrons and light absorption of catalysts. These findings may inspire peer researchers in developing new photocatalytic processes or in designing new photocatalysts for clean chemicals synthesis.

Graphical Abstract



Keywords Photocatalysis · Nanoparticles · Aromatic compounds · Selectivity regulation · Plasmonic effect

1 Introduction

Controlling selectivity in clean chemicals synthesis is crucial to obtaining target products with high purity [1, 2], and it is more challenging in cascade reactions [3, 4]. Apart from optimizing reaction kinetics and mass transfer kinetics to achieve better catalytic efficiency [5], developing new heterogeneous catalysts requires controlling active sites (e.g. composition, orientation, and distribution) [6, 7], and

✉ Xingguang Zhang
x.g.zhang@njfu.edu.cn
✉ Jianfeng Yao
jfyao@njfu.edu.cn
✉ Xuebin Ke
x.ke@hull.ac.uk

Extended author information available on the last page of the article

structures (e.g. pores, sizes, and shapes) [1, 8]. Electrons (e.g. density, interaction, and transfer) also play an indispensable role in manipulating catalytic performances, particularly in photocatalysis which involves light-excited electrons [9, 10]. In parallel, strategies associated with energy input are developed to enhance product selectivity, such as the use of microwave, ultrasound, an additional electric or electromagnetic field, and light irradiation [11–13].

Photocatalysis offers a promising opportunity to obtain a high product selectivity due to its capacity to influence catalytic reactions at ambient temperatures. More significantly, the unique property of incident light interacting with reactants or photocatalysts is able to initiate or accelerate reactions with low energy barriers and to give a certain product [14–17]. Recent studies demonstrate that plasmonic photocatalysts based on the localized surface plasmon resonance (LSPR) effect can actually achieve these goals [18–20]. The LSPR effect features a collective and coherent oscillation of the free conduction electrons with the incident photons on the surface of metal nanoparticles (NPs) [21–23]. These strong oscillating electrons can drive the target reaction locally (around active sites) and affect the product selectivity fundamentally [24–26]. However, the functional mechanism of light irradiation to tune reactive procedure remains ambiguous.

Herein, a tuneable laser source and a solar simulator are used to explore the processing mechanism involving incident light, light absorption, electron excitation, electron transfer and activating the reactants to obtain targeted products. In clean chemicals synthesis, the catalytic hydrogenation of nitro compounds is an ideal process to produce amines, mainly azobenzene (other products of azoxybenzene and aniline can also be produced via this route) [14], and the catalytic oxidation of benzyl alcohol plays a significant role to produce aromatic aldehydes [27]. Conventional catalytic processes of these two consecutive reactions always necessitate complicated methodologies to minimize the production of side-products [28–31]. This study highlights that light irradiation over supported plasmonic gold catalysts [14, 32] can effectively tune the catalytic selectivity of the aforementioned two cascade reactions, with the net contribution depending upon light wavelength and intensity at a certain temperature.

2 Experimental

2.1 Raw Materials

Chemicals of chloroauric acid (99.999%, HAuCl_4), L-Lysine (98.0%), sodium borohydride (99.99%, NaBH_4), hydrochloric acid (37%, HCl), nitrobenzene (99.0%), potassium hydroxide (99.0%, KOH), isopropanol (99.5%), and azobenzene (98.0%), were purchased from Sigma-Aldrich. The inert gas of argon was from the BOC (99.99%). The cerium (IV) oxide

support (nanopowder, 99.95%, CeO_2) was also purchased from Sigma-Aldrich and used without further purification.

2.2 Catalyst Preparation

In a glass beaker with a magnetic stirring bar, 2.5 g of support powders, such as CeO_2 , were dispersed into the 100 ml of 3.8×10^{-3} mol/L HAuCl_4 aqueous solution. Subsequently, 20 ml of 0.53 mol/L lysine was added dropwise to the mixture under stirring, and after that the stirring was prolonged for 30 min. To this suspension, 10 ml of 0.35 mol/L NaBH_4 solution was added dropwise, followed by adding 10 ml of 0.3 mol/L hydrochloric acid (to achieve a pH 9.5). The mixture was stirred for 1 h and aged for 24 h. Then the solid was separated, washed firstly with 600 ml deionized water for three times in a 250-ml centrifuge bottle to remove the chlorine ions, and the residual solution was tested by 0.1 mol/L AgNO_3 solution and no AgCl precipitate was observed. The solids were collected, dried at 60 °C for 16 h, and used directly as the photocatalyst.

2.3 Photocatalytic Tests

The reaction was conducted in a 50 ml round-bottomed Pyrex glass flask with a sealed spigot and a magnetic stirrer. The reaction temperature was controlled by an air-conditioner within a sealed wooden box. The light intensity in the reaction position was set at 0.1 W/cm^2 and could be adjusted by changing the distance between the reactor and the light source. The wavelength range was tuned by using various glass filters to cut off the irradiation below a certain value of wavelength. A tuneable laser source (OPOTECK VIBRANT, 350 II) and a solar simulator (NEWPORT, 150 W) were used as light source, respectively.

Catalytic reduction of nitrobenzene was conducted under the argon (Ar) atmosphere. Typically, 3 mmol of nitrobenzene, 30 ml of isopropanol as solvent, and 3 ml of 0.1 mol/L KOH solution in isopropanol were mixed in the reactor, followed by adding 100 mg of the catalyst and purging with argon gas, and then stirred during reaction and illuminated with the light source.

Catalytic oxidation of benzyl alcohol was conducted under the oxygen (O_2) atmosphere. Typically, 3 mmol of benzyl alcohol was dissolved into 30 ml of isopropanol, and 3 ml of 0.1 mol/L KOH solution in isopropanol and 100 mg of the catalyst were added into the mixture. The mixture was stirred during reaction and illuminated with the light source.

During these reactions, 0.5 ml aliquots were collected at given irradiation time intervals and filtered through a Millipore filter (pore size 0.45 μm) to remove the catalyst particulates. Then flask was purged with Ar or O_2 again for more than 3 min to remove air and then sealed. The filtrates were analyzed by an Agilent 6890 gas chromatograph with the

HP-5 column. Quantities of the products and reactants were calculated from the peak areas of the compounds using calibration curves. An Agilent HP5973 mass spectrometer was used to determine and analyze the product compositions.

2.4 Characterization

TEM images were taken with a JEOL JEM-2100 transmission electron microscope employing an accelerating voltage of 200 kV. The specimens were sample powders deposited onto a copper microgrid coated with a holey carbon film. The element composition of some samples was determined by energy-dispersive X-ray spectroscopy attached on an FEI Quanta 200 scanning electron microscope (The average gold loading was 2.8 wt%). The diffuse reflectance UV–Vis spectra of the samples were recorded on a Cary 5000 spectrometer. The XPS data were recorded on an ESCALAB 250 spectrometer and Al K α radiation was used as the X-ray source. The C1s peak at 284.5 eV was used as a reference for the calibration of the binding energy scale.

3 Results and Discussion

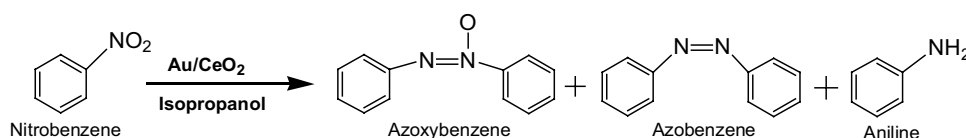
The catalytic performances of the hydrogenation of nitrobenzene are presented in Table 1. The effect of light irradiation on tuning the product selectivity is evident. In particular, at 40 °C and with the light off, the selectivity of azoxybenzene can be up to 91%; whereas with the light on, azoxybenzene disappears and the yield of azobenzene can be up to >99%.

At a higher temperature (80 °C), the influence of light is negligible and both light reaction and thermal reaction can achieve a complete conversion. Generally, the light irradiation can increase the reaction conversion compared with the reaction with light off at lower reaction temperatures and have significant influence on product selectivity, thereby playing a threshold/switch role in tuning the catalytic reaction procedure.

To explain this phenomenon, the physiochemical properties of catalysts are characterized by transmission electron microscopy (TEM), X-ray photoelectron spectroscopy (XPS), and UV–Vis spectroscopy. In Fig. 1a, the typical TEM images of the Au-NPs on the CeO₂ support show that Au NPs are well dispersed and have narrow size distributions within 2–6 nm. The XPS spectra (Fig. 1b) provides the spectra of Au 4f and confirms that the binding energies of Au4f_{7/2} and Au4f_{5/2} electrons are 84.0 and 87.7 eV, respectively, corresponding to the oxidation state of gold metal [33]. The UV–Vis spectra of Au/CeO₂ shows the absorption band centres at about 539 nm in wavelength owing to the LSPR effect; on the contrary, the CeO₂ support itself shows no absorption in the visible light region, which substantially demonstrates that the contribution of light irradiation to affecting the catalytic activity and selectivity via the LSPR effect of Au NPs only.

It would be exciting if the underlying mechanistic reasons for the light irradiation which affects catalytic selectivity are unravelled. At the current stage of this study, we propose that the distinct differences of reaction pathway at a certain reaction temperature can be ascribed to

Table 1 Catalytic performances of 3%Au/CeO₂ for selective reduction of nitrobenzene under the simulate sunlight source (a solar simulator)

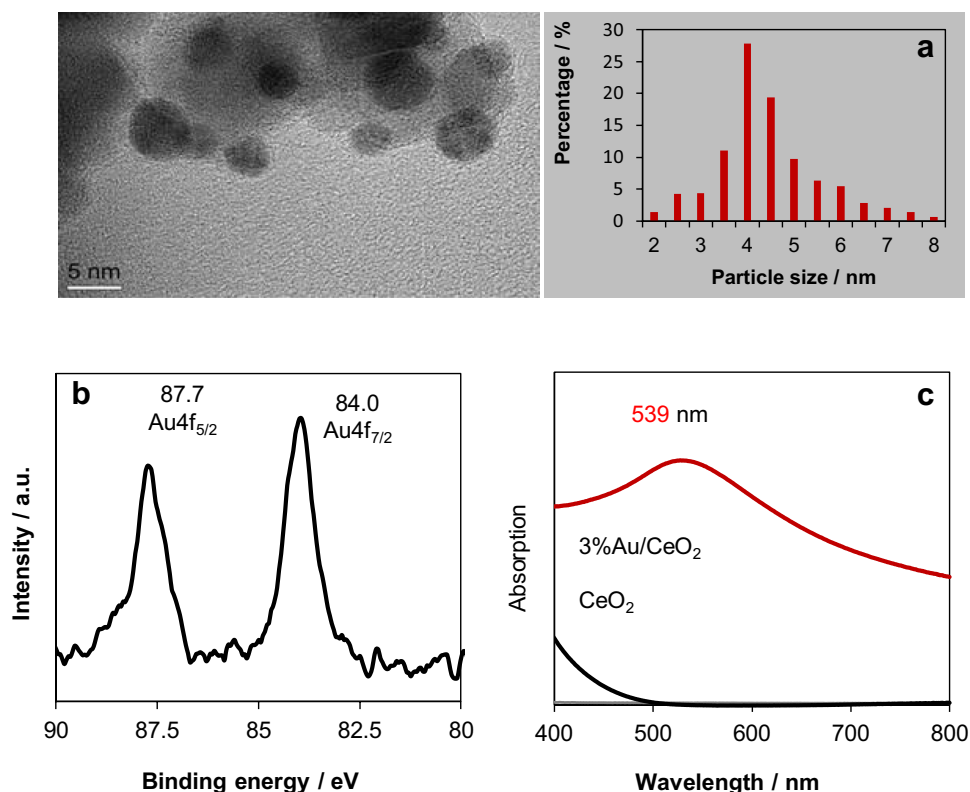


T (°C)	Light	Selectivity (%)			Conversion (%)	Net change (%)	
		Azoxybenzene	Azobenzene	Aniline		Nitrobenzene	Conversion
40	On	–	> 99	–	> 99	14	91
	Off	91	9	–	86		
60	On	–	96	4	> 99	7	90
	Off	92	6	2	93		
80	On	–	80	20	> 99	0	18
	Off	–	98	2	> 99		

Bold values highlight the catalytic results with light on

Reaction conditions time = 6 h, solvent = isopropanol (30 ml), catalyst = 3%Au/CeO₂ (100 mg), reactant = nitrobenzene (3 mmol), KOH (0.1 mol/L, 3 ml), light wavelength (full), and light intensity (0.1 W/cm²). *Control experiments* no products were detectable over the CeO₂ support as catalyst

Fig. 1 **a** TEM images of 3%Au/CeO₂ with Au size distribution, **b** XPS spectra and **c** UV-Vis spectra of 3%Au/CeO₂



“the reduction barriers of intermediate products” and “the light-induced electrons interaction” between reactant molecules and Au NPs, and these proposed associations have been initially explored in our previous studies [24, 25, 34]. To illustrate, the reduction of nitrobenzene can be induced by both heat and the light irradiation over supported gold catalysts [14, 28], undergoing different reaction pathways and thus giving different product selectivity. In the light-induced process, the solvent of isopropanol also serves as a hydrogen donor to form the intermediate species of Au–H bonds [14], and these species can break the N–O bonds to reduce nitrobenzene. Meanwhile, the resonating electrons of Au NPs strongly interact with the electrophilic nitro groups of nitrobenzene to facilitate the cleavage of

the N–O bonds by Au–H species. For these reasons, even at a lower temperature of 40 °C, the reduction of nitrobenzene still occurs efficiently; however, at a higher temperature of 80 °C, both heat and light irradiation take effect, and it is difficult to identify the individual contribution of heat or light, thereby showing identical conversions and similar selectivity. Hence, the similar experimental results at 80 °C with light on and off convince the switch role of light irradiation at lower reaction temperatures of 60 °C and 40 °C (Table 1).

As the light irradiation essentially affects the catalytic reaction procedure, then it is sensible to deduce that the catalytic performances should differ with the light source, light absorption and energy transfer. It is shown in Fig. 2a that the

Fig. 2 **a** The change in selectivity with the laser wavelength under the same light intensity of 80 mW/cm²; **b** the change in the product selectivity with the laser intensity at the same wavelength of 539 nm. AZY azobenzene, azoxy azoxybenzene

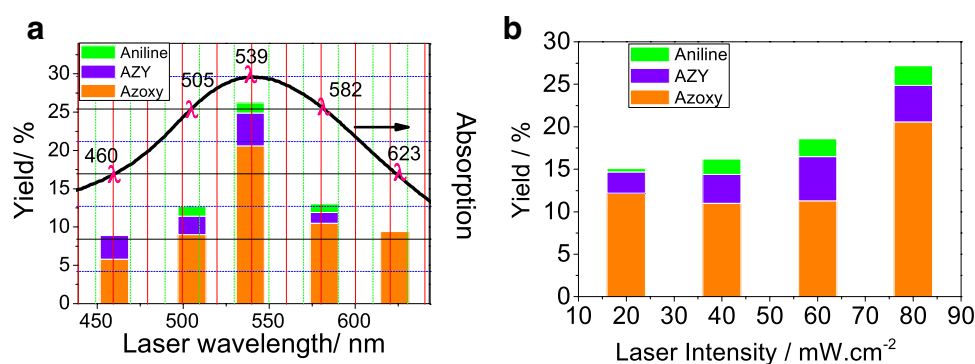
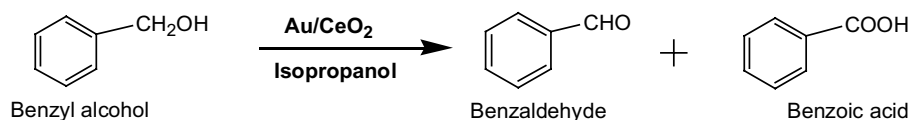


Table 2 Catalytic performances of 3% Au/CeO₂ for the selective oxidation of benzyl alcohol under simulate light source (a solar simulator)

T (°C)	Light	Selectivity (%)		Conversion (%) Benzyl alcohol	Net change (%)	
		Benzaldehyde	Benzoic acid		Conversion	Benzaldehyde
40	On	> 99	–	90	31	–
	Off	> 99	–	59		
60	On	91	9	97	28	9
	Off	> 99	–	69		
80	On	–	> 99	> 99	6	93
	Off	93	7	93		

Bold values highlight the catalytic results with light on

Reaction conditions time = 6 h, solvent = isopropanol (30 ml), catalyst = 3% Au/CeO₂ (100 mg), reactant = benzyl alcohol (3 mmol), KOH (0.1 mol/L, 3 ml), light wavelength (full), and light intensity (0.1 W cm²). *Control experiments* no products were detected over CeO₂ as catalysts

selectivity towards azoxybenzene, azobenzene and aniline varies as the function of light wavelength under the same light intensity. But the ability of incident light to excite energetic electrons decreases with longer wavelength and thus the reaction activity declined. The excited electron distributions are different even with the same (macroscopic) light intensity. In general, with the shorter wavelength, there have more electrons in a high energy level. For instance, with the same light absorption, at 505 and 582 nm, the conversions are roughly the same, but the reaction proceeds to different stages, namely, the selectivity is different. In the case of 460 and 623 nm, the latter only proceeds at the initial stage, having a > 99% of selectivity towards azoxybenzene.

Besides light wavelength, the light intensity also has influence on the catalytic selectivity as shown in Fig. 2b. Increasing light intensities at the fixed wavelength (at 539 nm) boost more energetic electrons, thus resulting in different product selectivity; the conversions also increase and undergo latter stages, that is, much higher yields of azobenzene and aniline are obtained.

Further to test the generality of this finding that light irradiation can tune the product selectivity, the selective oxidation of benzyl alcohol to benzaldehyde and then to benzoic acid was also investigated, and the catalytic results are shown in Table 2. At 40 °C, the oxidation of benzyl alcohol mainly produces benzaldehyde, but the conversion is much higher under visible light irradiation. On the other hand, the heat effect is significant at 80 °C, and benzyl alcohol is oxidized into benzaldehyde with light off, but it further transforms to benzoic acid if the light irradiation applies; these results show that the light irradiation acts as a “switch”

to control the production of benzaldehyde or benzoic acid at 80 °C. This observation is inspiring because it not only proves the “switch role” of light irradiation for these two selected representative cascade reactions but also demonstrates that this phenomenon applies to both reductive and oxidative cascade reactions.

4 Conclusion

This study highlights the contribution of light irradiation to tuning the selectivity of redox cascade reactions by means of supported plasmonic gold photocatalysts. The reduction of nitrobenzene and the oxidation of benzyl alcohol exhibit different selectivity with light on and off at a certain temperature. The net contribution correlates to light wavelength and intensity. To further identify or even quantify the contribution of light irradiation and to clarify their underlying mechanisms, more investigation will be performed on such as photocatalysts with different gold loadings or sizes and other redox cascade reactions. Overall, this study presents a promising approach to refining the product selectivity in clean chemicals synthesis, and could inspire the design of new catalytic materials and processes.

Acknowledgements We thank the National Natural Science Foundation of China (NNSFC 21706134), the Young Natural Science Foundation of Jiangsu province (BK20170918) and Natural Science Key Project of the Jiangsu Higher Education Institutions (15KJA220001) for financial support.

References

- Smit B, Maesen TLM (2008) *Nature* 451:671–678
- Climent MJ, Corma A, Iborra S (2011) *Chem Rev* 111:1072–1133
- Sun J, Karim AM, Li XS, Rainbolt J, Kovarik L, Shin Y, Wang Y (2015) *Chem Commun* 51:16617–16620
- Faisca Phillips AM, Pombeiro AJL, Kopylovich MN (2017) *ChemCatChem* 9:217–246
- Fan J, De bruyn M, Budarin VL, Gronnow MJ, Shuttleworth PS, Breeden S, Macquarrie DJ, Clark JH (2013) *J Am Chem Soc* 135:11728–11731
- Tomás RAF, Bordado JCM, Gomes JFP (2013) *Chem Rev* 113:7421–7469
- Zhang X, Wilson K, Lee AF (2016) *Chem Rev* 116:12328–12368
- Parlett CMA, Isaacs MA, Beaumont SK, Bingham LM, Hondow NS, Wilson K, Lee AF (2016) *Nat Mater* 15:178–182
- Kou J, Lu C, Wang J, Chen Y, Xu Z, Varma RS (2017) *Chem Rev* 117:1445–1514
- Liu H, Jiang T, Han B, Liang S, Zhou Y (2009) *Science* 326:1250–1252
- Kappe CO, Pieber B, Dallinger D (2013) *Angew Chem Int Ed* 52:1088–1094
- Baig RBN, Varma RS (2012) *Chem Soc Rev* 41:1559–1584
- Qu Y, Duan X (2013) *Chem Soc Rev* 42:2568–2580
- Zhu H, Ke X, Yang X, Sarina S, Liu H (2010) *Angew Chem* 122:9851–9855
- Marimuthu A, Zhang J, Linic S (2013) *Science* 339:1590–1593
- Tanaka A, Nishino Y, Sakaguchi S, Yoshikawa T, Imamura K, Hashimoto K, Kominami H (2013) *Chem Commun* 49:2551–2553
- Yang X-J, Chen B, Zheng L-Q, Wu L-Z, Tung C-H (2014) *Green Chem* 16:1082–1086
- Wang F, Li C, Chen H, Jiang R, Sun L-D, Li Q, Wang J, Yu JC, Yan C-H (2013) *J Am Chem Soc* 135:5588–5601
- Liu L, Ouyang S, Ye J (2013) *Angew Chem Int Ed* 52:6689–6693
- Ke X, Sarina S, Zhao J, Zhang X, Chang J, Zhu H (2012) *Chem Commun* 48:3509–3511
- Linic S, Christopher P, Ingram DB (2011) *Nat Mater* 10:911–921
- Christopher P, Xin H, Marimuthu A, Linic S (2012) *Nat Mater* 11:1044–1050
- Ueno K, Misawa H (2013) *J Photochem Photobiol C* 15:31–52
- Zhang X, Ke X, Zhu H (2012) *Chem Eur J* 18:8048–8056
- Zhang X, Du A, Zhu H, Jia J, Wang J, Ke X (2014) *Chem Commun* 50:13893–13895
- Zhang X, Ke X, Yao J (2018) *J Mater Chem A* 6:1941–1966
- Sankar M, Nowicka E, Carter E, Murphy DM, Knight DW, Bethell D, Hutchings GJ (2014) *Nat Commun* 5:3332
- Grirrane A, Corma A, García H (2008) *Science* 322:1661–1664
- Takenaka Y, Kiyosu T, Choi J-C, Sakakura T, Yasuda H (2009) *Green Chem* 11:1385–1390
- Corma A, Concepción P, Serna P (2007) *Angew Chem Int Ed* 46:7266–7269
- Grirrane A, Corma A, Garcia H (2010) *Nat Protocols* 11:429–438
- Ke X, Zhang X, Zhao J, Sarina S, Barry J, Zhu H (2013) *Green Chem* 15:236–244
- Khatri OP, Murase K, Sugimura H (2008) *Langmuir* 24:3787–3793
- Zhang X, Ke X, Du A, Zhu H (2014) *Sci Rep* 4:3805

Affiliations

Xingguang Zhang¹ · Jianfeng Yao¹ · Xuebin Ke²

¹ College of Chemical Engineering, Jiangsu Key Lab for the Chemistry & Utilization of Agricultural and Forest Biomass, Nanjing Forestry University, Nanjing 210037, Jiangsu, People's Republic of China

² School of Engineering and Computer Science, University of Hull, Hull HU6 7RX, UK